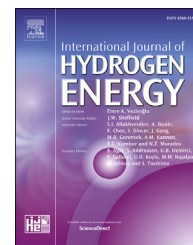




ELSEVIER

Available online at www.sciencedirect.com

ScienceDirect

journal homepage: www.elsevier.com/locate/hydro

A high-specific-energy magnesium/water battery for full-depth ocean application

Qianfeng Liu ^{a,b,1}, Zhao Yan ^{a,b,1}, Erdong Wang ^{a,*}, Suli Wang ^a,
Gongquan Sun ^{a,**}

^a Division of Fuel Cell & Battery, Dalian National Laboratory for Clean Energy, Dalian Institute of Chemical Physics, Chinese Academy of Sciences, Dalian 116023, Liaoning, China

^b University of Chinese Academy of Sciences, Beijing, 100039, China

ARTICLE INFO

Article history:

Received 14 March 2017

Received in revised form

19 July 2017

Accepted 19 July 2017

Available online 8 August 2017

Keywords:

Magnesium/water battery

Hydrogen evolution reaction

Underwater application

High pressure

Magnesium alloy

ABSTRACT

In this work, a high-specific-energy magnesium/water battery (Mg/H₂O battery) combining Mg oxidation with hydrogen evolution reaction (HER) is developed for full-depth ocean application. With the optimized platinum loading associated with moderate Ni(OH)₂ on nickel foam, the performance can be increased obviously. Coupled with AZ91 Mg alloy anode, the specific energy of Mg/H₂O battery reaches a dramatic value of 1003 W h kg⁻¹. Moreover, ultrahigh pressure of 1100 bar in the deep-sea simulated condition brings negligible effects on the performance of battery and electrodes. The influence of low temperature can be reduced to an acceptable level under the application at low discharge current density. Stable discharge of the battery for 100 days is also obtained. This work provides a new idea to supply power source with high specific energy, excellent environment adaptability, good safety and low cost for underwater application.

© 2017 Hydrogen Energy Publications LLC. Published by Elsevier Ltd. All rights reserved.

Introduction

With the increasing of ocean exploration in scientific research, resource utilization and military defense, a large number of devices, such as the autonomous or unmanned underwater vehicles (AUVs or UUVs) [1], manned submersible [2,3] and deep-sea lander [4], have been for underwater application. Along with these devices, the power sources [5–8] with high specific energy and good environmental adaptability are especially urgent due to the extreme conditions of

high pressure and low temperature [9,10] for long operation time in the deep-sea application [11]. The depth of the deepest ocean is about 11,000 m, where the pressure is roughly 1100 bar. Such a high pressure may destroy the battery structure and lower the discharge performance [12]. To avoid the pressure influence, thick pressure-proof hulls were used to protect the batteries [13]. However, the specific energy of power sources would be reduced obviously owing to the extra weight. Developing a seawater utilization battery with open construction is one of effective approaches to solve the problem above.

* Corresponding author.

** Corresponding author.

E-mail addresses: edwang@dicp.ac.cn (E. Wang), gqsun@dicp.ac.cn (G. Sun).

¹ These authors contributed equally to this work.

<http://dx.doi.org/10.1016/j.ijhydene.2017.07.157>

0360-3199/© 2017 Hydrogen Energy Publications LLC. Published by Elsevier Ltd. All rights reserved.

The Mg is an excellent electrode material due to its high specific capacity (2200 mA h g^{-1}), low cost, and good electrochemical activity in seawater [14,15]. Thus, Mg-based batteries are appropriate to the ocean environment [16]. Many kinds of Mg-based batteries had been explored, such as magnesium seawater activated battery [17], magnesium/hydrogen peroxide semi-fuel cell [18] and magnesium/dissolved oxygen battery [19,20]. Among above batteries, the magnesium/dissolved oxygen battery is the only one that takes oxidant from seawater. Therefore, the magnesium/dissolved oxygen battery with high specific energy and relatively simple structure have been applied successfully in the deep-sea [21]. However, the concentration of the dissolved oxygen in the ocean is low and uneven [11], which seriously reduces its volume power density and limits its application in the broad ocean.

Using water as the cathode oxidant directly seems to be an attractive idea to overcome the troubles caused by the concentration limitation of dissolved oxygen of the magnesium/dissolved oxygen battery. Such a battery can be denominated as Mg/H₂O battery (Fig. 1), as the other metal/water batteries [22,23]. On account of that hydrogen is produced on cathode, this battery was designed as a hydrogen generator for PEMFCs [24]. However, Mg/H₂O battery can be a promising power source [25] by itself because its theoretic specific energy reaches 4090 W h kg^{-1} .

To achieve a better performance for Mg/H₂O battery, decreasing the cathode polarization of HER and increasing the anode current efficiency respectively, are of great importance. Although platinum modified nickel foams (Pt–NF) prepared by facile chemical [26,27] or electrochemical [28] deposition are widely used for HER electrodes, the electrochemical performance of HER is poor with low Pt loading [27,29]. Subbaraman et al. [30–32] found that moderate Ni(OH)₂ modified Pt can obviously enhance the HER electrocatalytic activity in alkaline condition. Besides, the surface of NF can be oxidized into Ni(OH)₂ under wet condition [33], and the quantity of Ni(OH)₂

can be controlled by the oxidation time [34]. In this way, the cathode loading of Pt may be decreased when the Pt–NF electrode modified with moderate Ni(OH)₂ [35,36]. In the case of anode, a higher current efficiency and a more negative potential are preferred to attain a higher specific energy of the Mg/H₂O battery. However, the current efficiency of pure Mg is too low (~13%) for the battery under long time discharge [20]. Compared with pure Mg, the AZ-series Mg alloys (AZ alloys) are of great corrosion resistance in seawater [37] or under high current density [17]. Nevertheless, the anode efficiencies of AZ alloys are undefined at low current density during long operation time in seawater. Accordingly, it is valuable to construct the Mg/H₂O battery with adequate electrodes materials.

In this work, we fabricated Mg/H₂O batteries with simple structure using pure Mg or AZ alloys as the anodes and Pt–NF as the cathode. The performance of Mg/H₂O batteries using different anodes and cathodes was evaluated. Then, the anode efficiencies, as well as the effects on the battery specific energy were investigated in detail. After that, the influences of the pressure and temperature similar to the extreme condition of the deep-sea on the battery, electrodes and electrolyte, respectively, were discussed to determine the major factor affecting the battery performance. Finally, a longtime discharge was carried out to test the stability of the battery.

Experimental

Preparation and characterization of electrodes

The cathode (Pt–NF) was prepared by a simple chemical deposition method. The nickel foam (thickness: 1.7 mm, surface density: 320 g m^{-2} , Tianyu Technology, Shandong) was cut into $20 \times 50 \text{ cm}^2$ firstly, then immersed in 1 mol L^{-1} HCl for 60 min, and washed with deionized water (DI water) for three times, then immediately immersed in 500 mL aqueous

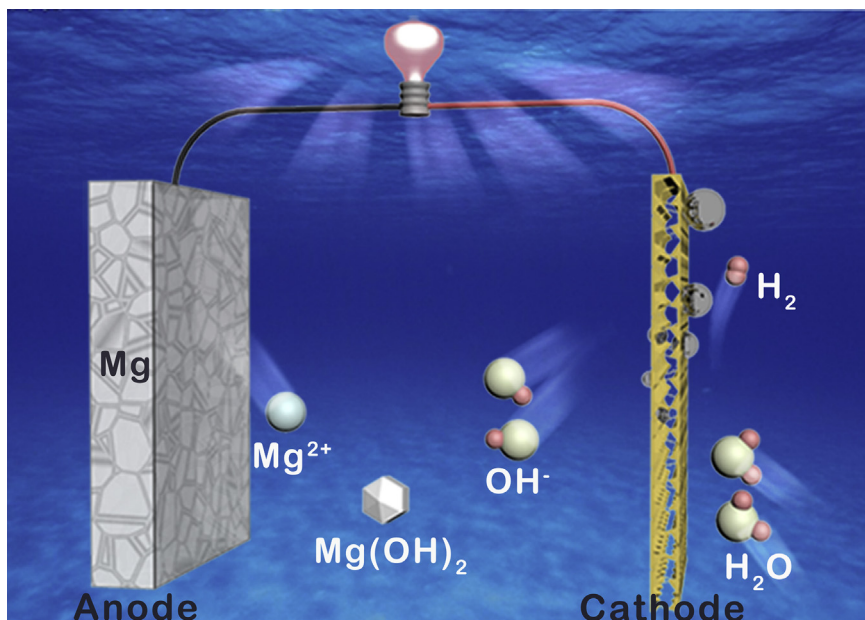


Fig. 1 – The structure and working principle of Mg/H₂O battery.

solution of 0.5 mmol L⁻¹ H₂PtCl₆ and 5 mmol L⁻¹ HCl for 24 h under 20 ± 1 °C. Finally, it was washed by DI water three times and dried under ambient temperature for 12 h. The anodes (Shanxi Yinguang Magnesium Ltd. China) of pure Mg and AZ alloys (AZ31, AZ61 and AZ91 prepared by rolling technology) were cut into designed size and polished before use.

The cathode loading of Pt (40.5 ± 0.2 μg cm⁻²) and the chemical composition of the anodes listed in Table 1 were measured by inductive coupled plasma emission spectrometer (ICP-OES, PerkinElmer, 7300DV). The morphology of the cathodes before and after pressure treatment was characterized by scanning electron microscope (SEM, JSM-7800F).

Electrochemical measurement of electrodes and Mg/H₂O batteries

The electrodes were tested in the three-electrode electrochemical cell setup with saturated calomel electrode (SCE) as the reference electrode, a stainless steel sheet as the counter electrode and 3.5 wt% NaCl solution as the electrolyte using an electrochemical workstation (1287A and 1260A, Solartron). The work electrode was the cathode with a working area of 1 × 1 cm² (cut from the large cathode as made) or the anode with 0.5 × 0.5 cm². The current density was normalized by geometrical area of the electrodes. The holding time of galvanostatic method for each current value was 120 s except for anodes pressure experiment (1000 s).

Mg/H₂O batteries tests were performed by home-made Mg/H₂O cells with 3.5 wt% NaCl electrolyte solution as a substitution for seawater using the Battery Testing System (BTS-5V50 mA and BTS-5V500 mA, Neware). The cathode (working area of 2 × 2 cm² which is the same to the anode) was cut from the large one as described before. The distance between cathode and anode was 2.0 ± 0.1 mm except for the pressure experiments (3.3 ± 0.1 mm). The operation temperature for the polarization tests was controlled (15 ± 1 °C) while the constant current discharge of the batteries was conducted under ambient temperature (15 ± 4 °C). The electrochemical impedance spectroscopy (EIS) measurements were conducted at 0.6 V for the batteries with the frequency ranging from 100 kHz to 0.1 Hz and AC voltage amplitude of 5 mV.

The batteries pressure tests were performed via the deep-sea ultrahigh pressure simulation test device (Maximum pressure: 1300 bar, Institute of Deep-sea Science and Engineering, Chinese Academy of Science). The batteries and related electrodes were put into an airtight rubber box filled with 3.5 wt% NaCl solution. The supplied pressure for the battery was from 1 bar to 10, 30, 100, 300 and 1100 bar, finally, backed to 1 bar (The pressure of 1 bar is the value of

atmosphere, which is not supplied by the device.). Under each pressure, the polarization and discharge performances were tested.

Results and discussion

Performance of electrode materials

In order to heighten the battery performance, Pt–NF cathode with the Pt loading of 40.5 ± 0.2 μg cm⁻² and different anodes (pure Mg or AZ alloys) were used as the electrode materials, and the polarization curves and the corresponding power density plots of the Mg/H₂O batteries are presented in Fig. 2. It can be seen from Fig. 2a that the battery with the Pt–NF cathode exhibits an obviously better performance (10.5 mW cm⁻² at 40 mA cm⁻²) compared with that of the NF cathode (3.3 mW cm⁻² at 20 mA cm⁻²). The battery voltage at 1 mA cm⁻² is around 0.61 V when the Pt–NF cathode and AZ61 anode are used. It should be noted that the open circuit voltage (OCV) is probably not accurate resulting from the existence of dissolved oxygen in the electrolyte [24]. Like traditional magnesium seawater batteries [19,38], excellent seawater corrosion resistance for the anode of Mg/H₂O battery is sorely required. It had been proved by previous references [37,39,40] that commercial AZ alloys manufactured by rolling technology exhibit low self-corrosion rate and high corrosion potential, which are suitable to serve as the anodes of the Mg/H₂O batteries. Herein, we constructed Mg/H₂O batteries with different AZ alloys as the anode paired with the Pt–NF cathode. Compared with pure Mg anode, the battery performance with the anodes of AZ alloys is decreased as shown in Fig. 2b. The voltage of the battery with pure Mg anode is around 0.75 V at 1 mA cm⁻², which is much higher than that of AZ alloy anodes. However, the voltage differences are reduced with the increase of current density.

The galvanostatic discharge performance, anode efficiency and the specific energy of the Mg/H₂O batteries with different anodes are shown in Fig. 3. To reduce the effect of the dissolved oxygen in the electrolyte on the OCV, the batteries were discharged at 2.5 mA cm⁻² for 2 min to deplete the dissolved oxygen prior to the regular tests. As shown in Fig. 3a and b, the voltage of battery with pure Mg is higher than those of AZ alloys for about 80–100 mV at both current density of 1.0 mA cm⁻² and 2.5 mA cm⁻² throughout the discharge process, resulting from the mixed potential generated by the formation of alloy phases in the anode. It is also pointed out that the voltage waves of about 30 mV during the discharge are associated with the operation temperature. As mentioned above, anode efficiency is crucial to the specific energy of the

Table 1 – Chemical composition (wt%) of pure Mg, AZ31, AZ61 and AZ91 Mg alloys according to ICP-OES.

Materials	Al	Zn	Mn	Si	Cu	Ni	Fe	Mg
Pure Mg	0.003	0.006	0.0039	0.003	0.003	0.0007	0.0047	Balance
AZ31	3.05	0.82	0.40	0.02	0.003	0.0012	0.0023	Balance
AZ61	6.20	0.74	0.23	0.04	0.003	<0.001	0.004	Balance
AZ91	8.80	0.71	0.19	0.029	0.002	<0.001	0.001	Balance

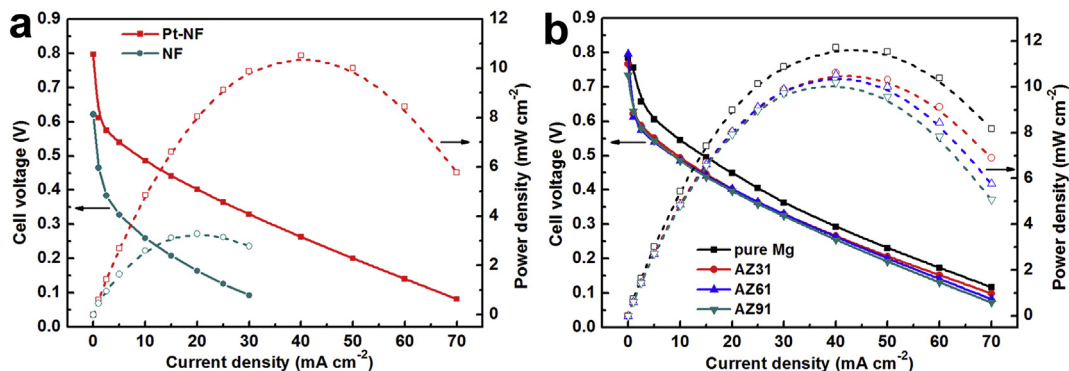


Fig. 2 – Polarization curves and corresponding power density plots of Mg/H₂O batteries. (a) AZ61 as the anode with different cathodes. (b) Pt–NF as the cathode with different anodes.

Mg/H₂O battery. The anode efficiency is calculated by the traditional weight-loss method, and the theoretical capacities for pure Mg and AZ alloys during the calculation are all regarded as 2200 mA h g⁻¹.

From Fig. 3c, it can be seen that the anode efficiency increases with the increase of aluminum content in AZ alloys as the battery discharged at 2.5 mA cm⁻² for 120 h. The maximum efficiency of the anodes is 85.0% obtained from AZ91, which is much higher than that of pure Mg (38.3%). As the battery discharged at a smaller current density of 1 mA cm⁻² for 250 h, the efficiencies of pure Mg and AZ91 are sharply decreased compared with those discharged at 2.5 mA cm⁻², but similar results are not observed for AZ31 and

AZ61. This might be explained that more severe hole-corrosion occurred for pure Mg and AZ91 anode due to their metallographic structure during longtime discharge with relatively low current [41,42]. Fig. 3d shows the specific energy of the Mg/H₂O batteries with different anodes. As the discharge voltages of batteries with different anodes are very close, the battery specific energy is strongly relevant to anode efficiency. As shown in Fig. 3d, the specific energy of the Mg/H₂O battery with pure Mg anode is quite low due to its poor efficiency, although the battery voltage is much higher. In contrast, a dramatically high specific energy of 1003 W h kg⁻¹ is achieved for the battery with AZ91 alloy anode. Such an exciting result and the low cost of \$0.011 W h⁻¹ (Table S1)

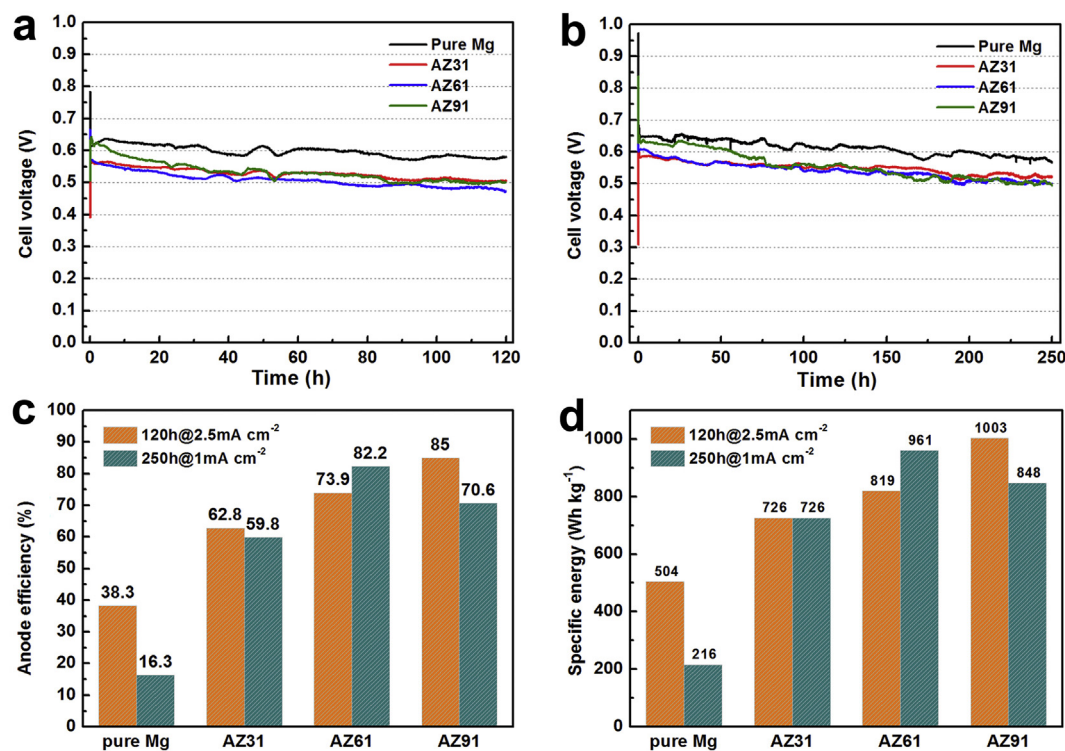


Fig. 3 – Discharge performance, anode efficiency, and specific energy of Mg/H₂O batteries using different anodes. (a) Discharge curves at 2.5 mA cm⁻² for 120 h. (b) Discharge curves at 1.0 mA cm⁻² for 250 h. (c) Anode efficiencies and (d) specific energies of Mg/H₂O batteries.

prove that the Mg/H₂O battery can be a competitive power source for undersea application.

The influence of pressure

Based on the Nernst equation, the theoretical equilibrium voltage of the Mg/H₂O battery will decrease with the increase of hydrogen pressure caused by the seawater pressure in the deep-sea. The voltage drop is:

$$\Delta E = 29.5 \text{ mV} \times \log (P/\text{bar}) \quad (1)$$

Accordingly, if the Mg/H₂O battery worked at 10,000 m below sea level, the equilibrium voltage will decrease by 88.5 mV. However, the real effect of the pressure on the battery performance is unclear as the complicated real conditions on the electrodes and the electrolyte [43,44]. Here, an ultrahigh pressure device, which simulates the full-depth ocean condition with the pressure ranging from 1 bar (0 m) to 1100 bar (11,000 m), was used to evaluate the detailed effects of pressure on the performance of battery and electrodes. To exclude the non-pressure factors, such as the battery self-degradation and the temperature change, two same batteries were tested simultaneously under the same conditions except for the pressure. Fig. 4a and b shows the performance comparison of the batteries under different pressure with the AZ61 anode (pure Mg and other AZ alloy anodes exhibited the similar behaviors, Fig. S1 and S2). It can be seen from Fig. 4a that the voltage difference under the

pressure of 1 bar and 1100 bar is very small in the low current density region. However, unexpectedly, the battery showed a remarkable performance increase under the pressure of 1100 bar compared to that of 1 bar at higher current density. This phenomenon might be explained by the effect of the volume change of the hydrogen bubbles. Under high pressure condition, the smaller bubbles will decrease the increment of the ohmic resistance of the electrolyte and the cathode polarization which are the main polarization determination in this battery at higher current density. In detail, the volume of hydrogen bubbles is roughly 1.1 cm³ as the battery discharges for 2 min at 20 mA cm⁻² under atmosphere pressure. In the case of the pressure of 1100 bar, the gas is compressed to 1.0 × 10⁻³ cm³. However, with continuous discharge, the bubbles will also accumulate and grow up as that of atmosphere, and the above advantage might be dropped.

From the discharge curves at 2.5 mA cm⁻² under different pressures (Fig. 4b), the voltage is stable with slight drops by the increase of pressure. The synchronous test under atmosphere pressure gives a close voltage level but a little different voltage change probably due to the morphology change of hydroxide layer on the anode surface arising from the pressure difference. Nevertheless, it is strongly proved that this Mg/H₂O battery can be used in the full-depth ocean.

To further verify the effect factor of voltage difference in high current density region, the anode and the cathode potentials were tested individually before and after the

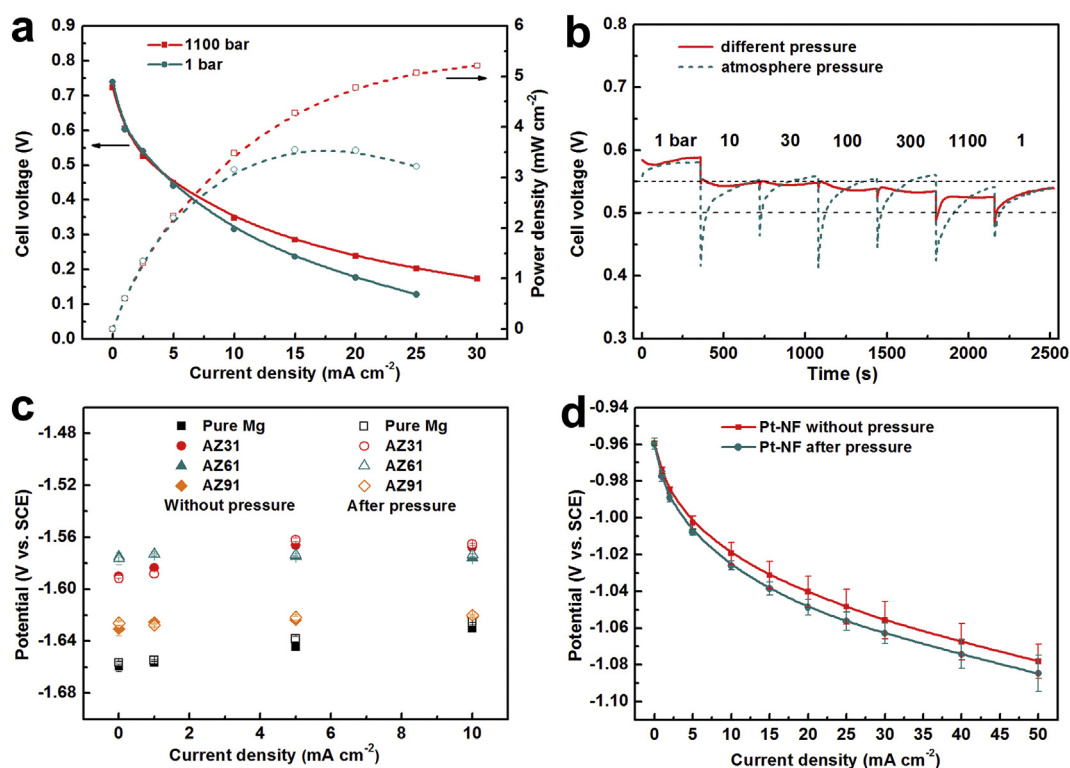


Fig. 4 – The influences of pressure on the batteries and electrodes. (a) Polarization performance under 1100 bar and 1 bar with AZ61 anode and Pt–NF cathode. (b) Discharge curves under different pressure and atmosphere pressure at 2.5 mA cm⁻² with AZ61 anode and Pt–NF cathode. (c) Potentials of the anodes before and after pressure test. (d) Potential curves of the cathodes before and after pressure test.

treatment at the pressure of 1100 bar. As shown in Fig. 4c, the potentials of anodes suffered from the pressure of 1100 bar are almost the same to that without pressure, which confirmed that the electrochemical property of anodes are not changed after the treatment of high pressure. As for the cathode, the little performance inferior can also be neglected (Fig. 4d). SEM images show that the cathode suffered from high pressure (Fig. 5b) contains more Ni(OH)₂ sheets than that without pressure (Fig. 5a). The abundant Ni(OH)₂ sheets on the surface of cathode may be caused by oxidation of the oxygen in the air during drying process after the contact with NaCl solution [33,34]. These results show excellent invariability of the anodes and cathodes under high pressure, which insures the excellent discharge performance of Mg/H₂O battery in deep-sea.

The influence of temperature

As an undersea power source, the effect of temperature of the ocean on the Mg/H₂O battery performance should be considered. The temperature is measured to be 0–4 °C in deep-sea [11], which will decrease the performance of battery due to the thermodynamics and kinetics reasons compared to that of ambient temperature. To the best of our knowledge, the HER performance of Pt-based electrodes in NaCl solution at near 0 °C has not studied yet. Thus, it is necessary to investigate the temperature influence on the Mg/H₂O battery to guide the battery design and further understand the HER in practical operation temperature.

Fig. 6 shows the influence of the temperature on the battery and electrodes. As shown in Fig. 6a, the battery voltages are 0.625, 0.606 and 0.571 V at 1.0 mA cm⁻² under the temperatures of 25 °C, 15 °C, and -1 °C, respectively. Correspondingly, the maximum power densities are 13.8 mW cm⁻², 10.7 mW cm⁻², and 6.7 mW cm⁻². The significant decrease of the performance causing by the temperature drop guides us that this battery should be operated in low current density region in deep-sea application.

In order to further distinguish the contribution of the decay caused by cathode, anode and electrolyte with the decrease of the temperature, we investigated the influence of temperature for the three components individually by means of EIS and the constant current polarization

technologies. From Fig. 6b, it is shown that the value of the charge-transfer impedance (R_{CT}) increases as the temperature decreases, which means low temperature leads to low electrode kinetics. In addition, the ohmic resistance of electrolyte (R_s) also increases as the temperature decrease, that is, 5.4, 6.4 and 8.8 Ω cm² when the temperature is 25, 15 and -1 °C. The calculated value of electrolytic conductivity is 0.043, 0.036 and 0.026 S cm⁻¹, which limits the discharge at high current density due to the significant polarization loss. The iR-correction polarization curves of electrodes were tested in a three-electrode cell and plotted in Fig. 6c. Considering the comparability, the holding time (120 s) is the same to battery tests. Although the polarization loss of cathode was greater (~120 mV at 25 °C from 0 to 50 mA cm⁻²) than anode AZ61 (pure Mg and other AZ alloy anodes exhibited the similar behaviors, Fig. S3), the main polarization loss for the battery is ohmic polarization of electrolyte at relatively high current density. For example, the potential difference of cathode and anode is 0.50 V at 50 mA cm⁻², but the battery actual voltage dropped to 0.28 V due to the potential loss arising from the electrolyte, which is much higher than those of the cathode and anode. More intuitive illustration is shown in Fig. 6d, in which the polarization difference of the cathode, anode and electrolyte were calculated by the potential difference between that of 25 and -1 °C.

The stability of Mg/H₂O battery

Based on the successful design of Mg/H₂O battery with ultra-high specific energy and excellent environmental adaptability, the stability was also evaluated under galvanostatic discharge of 1.0 mA cm⁻² for 100 days and presented in Fig. 7. It can be seen that the battery voltage decreases to 0.60 V as the load applied, and the voltage range is generally from 0.60 V to 0.42 V. It should be noted that the discharge voltage increases obviously due to the anode or electrolyte replacement during the test, which indicates that Mg/H₂O battery may exhibit a better performance in the undersea environment where the seawater electrolyte is abundant and regenerative. The above results prove that the Mg/H₂O batteries presented in this work can provide long operation time with the remarkably stable Pt–NF cathode.

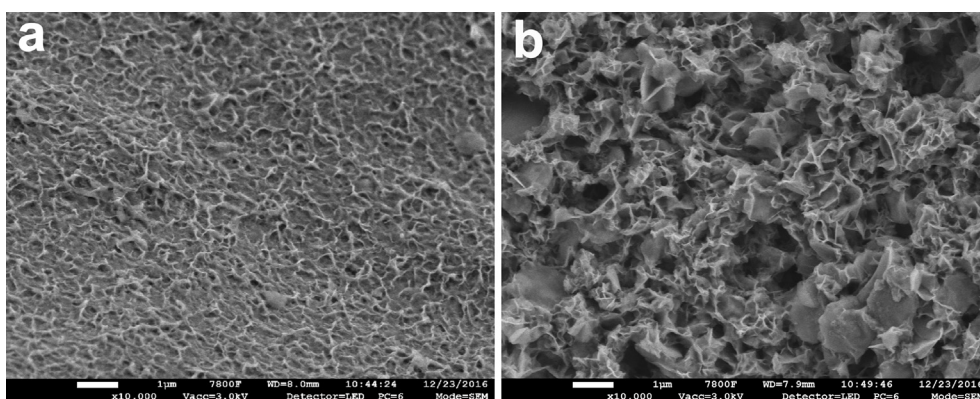


Fig. 5 – The SEM images of the cathodes (a) before and (b) after 1100 bar pressure test.

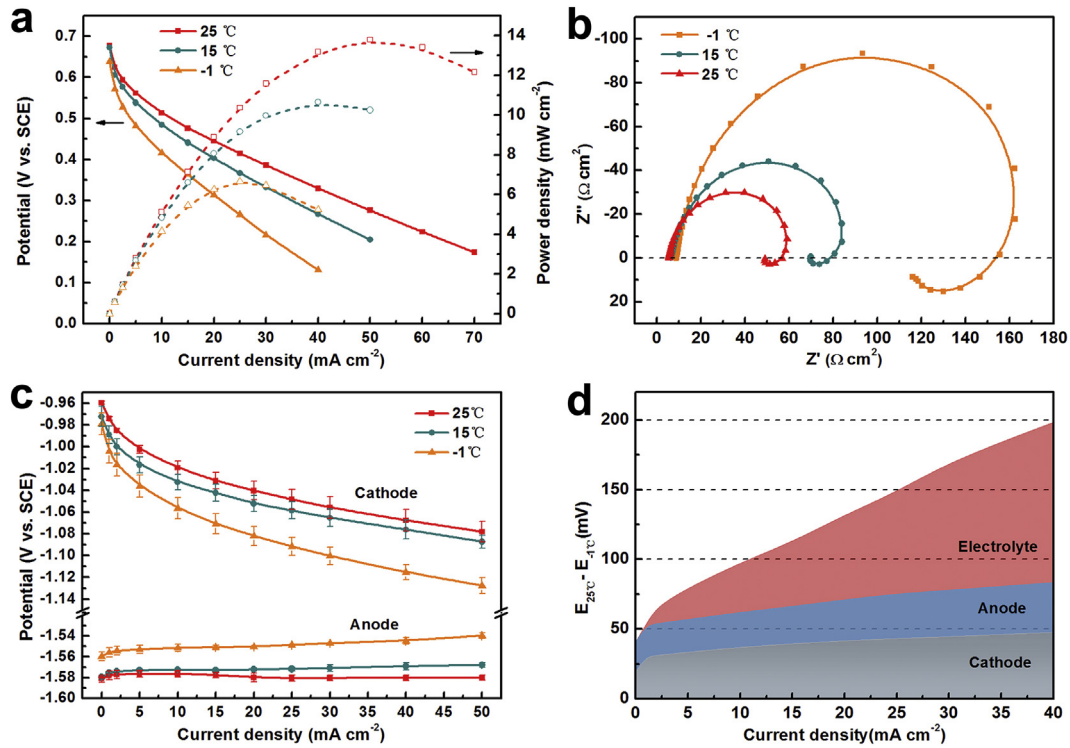


Fig. 6 – The influence of temperature for Mg/H₂O battery. (a) Polarization curves and (b) EIS of Mg/H₂O battery. (c) The temperature influence for electrodes polarization. (d) The polarization difference of electrodes and electrolyte caused by temperature change.

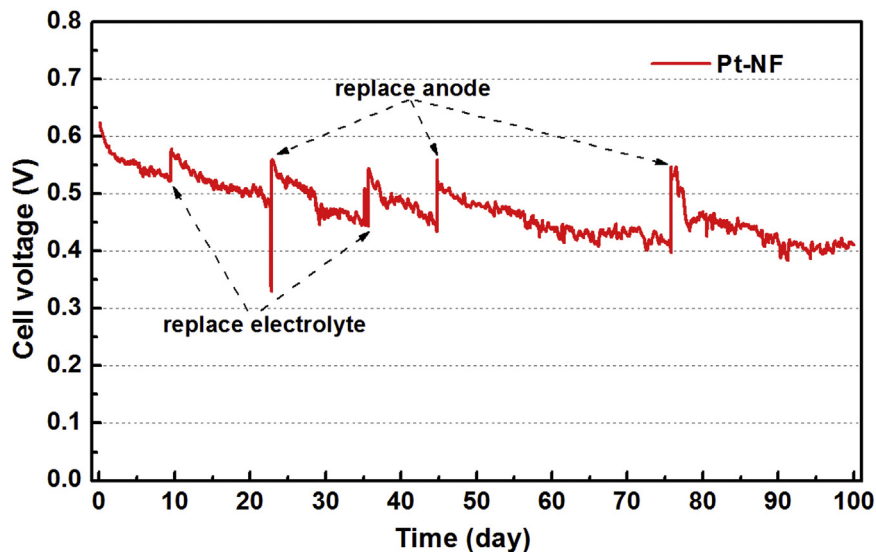


Fig. 7 – The stability test of Mg/H₂O battery with AZ61 anode and Pt–NF cathode under galvanostatic discharge of 1.0 mA cm⁻².

Conclusions

A high-specific-energy Mg/H₂O battery with the combination of Mg oxidation and HER was developed and investigated in this paper. By using AZ91 alloy anode, the battery exhibited an ultrahigh specific energy of 1003 W h kg⁻¹ and noticeable

anode efficiency of 85.0%. No obviously negative effects were detected to the Mg/H₂O battery at ultrahigh pressure of 1100 bar, which indicates that the battery can be used in the full depth of the broad ocean without complicated shells. The influence of low temperature in deep-sea on the polarization loss can be reduced to an acceptable degree by the design of low discharge current density. In addition, the battery showed

excellent stability during discharge test for nearly 100 days. All these results prove that the Mg/H₂O battery with high specific energy will be a promising power source for full-depth ocean application.

Acknowledgement

We gratefully acknowledge the financial support of this research by the Key Program of the Chinese Academy of Sciences (Grant No. KGZD-EW-T08), National Key Research and Development Program (Grant No. 2017YFC0306403), Strategic Priority Research Program of the Chinese Academy of Sciences (Grant No. xda13040101) and the Youth Innovation Promotion Association of the Chinese Academy of Sciences. We acknowledge the Institute of Deep-sea Science and Engineering, Chinese Academy of Science for the support of the deep-sea ultrahigh pressure simulation test device and the related technology.

Appendix A. Supplementary data

Supplementary data related to this article can be found at <http://dx.doi.org/10.1016/j.ijhydene.2017.07.157>.

REFERENCES

- [1] Wang X, Shang J, Luo Z, Tang L, Zhang X, Li J. Reviews of power systems and environmental energy conversion for unmanned underwater vehicles. *Renew Sustain Energy Rev* 2012;16:1958–70.
- [2] Lutz RA, Falkowski PG. A dive to challenger deep. *Science* 2012;336:301–2.
- [3] Kohnen W. Review of deep ocean manned submersible activity in 2013. *Mar Technol Soc J* 2013;47:56–68.
- [4] Jones EG, Collins MA, Bagley PM, Addison S, Priede IG. The fate of cetacean carcasses in the deep sea: observations on consumption rates and succession of scavenging species in the abyssal north-east Atlantic Ocean. *Proc Roy Soc Lond B Bio* 1998;265:1119–27.
- [5] Arges CG, Prabhakaran V, Wang L, Ramani V. Bipolar polymer electrolyte interfaces for hydrogen-oxygen and direct borohydride fuel cells. *Int J Hydrogen Energy* 2014;39:14312–21.
- [6] Hasvold Ø, Størkersen NJ. Electrochemical power sources for unmanned underwater vehicles used in deep sea survey operations. *J Power Sources* 2001;96:252–8.
- [7] Cai Q, Brett DJL, Browning D, Brandon NP. A sizing-design methodology for hybrid fuel cell power systems and its application to an unmanned underwater vehicle. *J Power Sources* 2010;195:6559–69.
- [8] Buckle JR, Knox A, Siviter J, Montecucco A. Autonomous underwater vehicle thermoelectric power generation. *J Underwater Mater* 2013;42:2214–20.
- [9] Pendergast DR, DeMauro EP, Fletcher M, Stimson E, Mollendorf JC. A rechargeable lithium-ion battery module for underwater use. *J Power Sources* 2011;196:793–800.
- [10] Doble MJ, Forrest AL, Wadhams P, Laval BE. Through-ice AUV deployment: operational and technical experience from two seasons of arctic fieldwork. *Cold Reg Sci Technol* 2009;56:90–7.
- [11] Kennish MJ. *Practical handbook of marine science*. 3rd ed. Boca Raton: CRC Press; 2000.
- [12] Hasvold Ø, Størkersen NJ, Forseth S, Lian T. Power sources for autonomous underwater vehicles. *J Power Sources* 2006;162:935–42.
- [13] Mendez A, Leo TJ, Herreros MA. Current state of technology of fuel cell power systems for autonomous underwater vehicles. *Energies* 2014;7:4676–93.
- [14] Bergthorson JM, Yavor Y, Palecka J, Georges W, Soo M, Vickery J, et al. Metal-water combustion for clean propulsion and power generation. *Appl Energy* 2017;186:13–27.
- [15] Uan JY, Yu SH, Lin MC, Chen LF, Lin HI. Evolution of hydrogen from magnesium alloy scraps in citric acid-added seawater without catalyst. *Int J Hydrogen Energy* 2009;34:6137–42.
- [16] Yu K, Huang Q, Zhao J, Dai YL. Electrochemical properties of magnesium alloy anodes discharged in seawater. *Trans Nonferrous Met Soc* 2012;22:2184–90.
- [17] Wang NG, Wang RC, Peng CQ, Hu CW, Feng Y, Peng B. Research progress of magnesium anodes and their applications in chemical power sources. *Trans Nonferrous Met Soc* 2014;24:2427–39.
- [18] Hasvold O, Johansen KH, Mollestad O, Forseth S, Størkersen N. The alkaline aluminium hydrogen peroxide power source in the Hugin II unmanned underwater vehicle. *J Power Sources* 1999;80:254–60.
- [19] Hasvold O, Lian T, Haakaas E, Størkersen N, Perelman O, Cordier S. CLIPPER: a long-range, autonomous underwater vehicle using magnesium fuel and oxygen from the sea. *J Power Sources* 2004;136:232–9.
- [20] Wilcock WSD, Kauffman PC. Development of a seawater battery for deep-water applications. *J Power Sources* 1997;66:71–5.
- [21] Shinohara M, Araki E, Mochizuki M, Kanazawa T, Suyehiro K. Practical application of a sea-water battery in deep-sea basin and its performance. *J Power Sources* 2009;187:253–60.
- [22] Katoh T, Inda Y, Nakajima K, Ye RB, Baba M. Lithium/water battery with lithium ion conducting glass-ceramics electrolyte. *J Power Sources* 2011;196:6877–80.
- [23] Shen PK, Tseung ACC, Kuo C. Design of a dome-shaped aluminum water battery. *J Appl Electrochem* 1994;24:145–8.
- [24] Hahn R, Mainert J, Glaw F, Lang KD. Sea water magnesium fuel cell power supply. *J Power Sources* 2015;288:26–35.
- [25] Xie P, Rong MZ, Zhang MQ. Moisture battery formed by direct contact of magnesium with foamed polyaniline. *Angew Chem Int Ed* 2016;55:1805–9.
- [26] Huang L, Hou Y, Yu Z, Peng Z, Wang L, Huang J, et al. Pt/Fe-NF electrode with high double-layer capacitance for efficient hydrogen evolution reaction in alkaline media. *Int J Hydrogen Energy* 2017;42:9458–66.
- [27] Kuleshov VN, Kuleshov NV, Grigoriev SA, Udriș EY, Millet P, Grigoriev AS. Development and characterization of new nickel coatings for application in alkaline water electrolysis. *Int J Hydrogen Energy* 2016;41:36–45.
- [28] Li M, Ma Q, Zi W, Liu X, Zhu X, Liu SF. Pt monolayer coating on complex network substrate with high catalytic activity for the hydrogen evolution reaction. *Sci Adv* 2015;1. <http://dx.doi.org/10.1126/sciadv.1400268>. e1400268.
- [29] Fiameni S, Herraiz-Cardona I, Musiani M, Perez-Herranz V, Vazquez-Gomez L, Verlatto E. The HER in alkaline media on Pt-modified three-dimensional Ni cathodes. *Int J Hydrogen Energy* 2012;37:10507–16.
- [30] Subbaraman R, Tripkovic D, Strmcnik D, Chang KC, Uchimura M, Paulikas AP, et al. Enhancing hydrogen evolution activity in water splitting by tailoring Li⁺-Ni(OH)₂-Pt interfaces. *Science* 2011;334:1256–60.
- [31] Danilovic N, Subbaraman R, Strmcnik D, Paulikas AP, Myers D, Stamenkovic VR, et al. The effect of noncovalent

- interactions on the HOR, ORR, and HER on Ru, Ir, and Ru_{0.50}Ir_{0.50} metal surfaces in alkaline environments. *Electrocatalysis* 2012;3:221–9.
- [32] Danilovic N, Subbaraman R, Strmcnik D, Chang KC, Paulikas AP, Stamenkovic VR, et al. Enhancing the alkaline hydrogen evolution reaction activity through the bifunctionality of Ni(OH)₂/metal catalysts. *Angew Chem Int Ed* 2012;51:12495–8.
- [33] Xiong X, Ding D, Chen D, Waller G, Bu Y, Wang Z, et al. Three-dimensional ultrathin Ni(OH)₂ nanosheets grown on nickel foam for high-performance supercapacitors. *Nano Energy* 2015;11:154–61.
- [34] Lee J, Lim GH, Lim B. Nanostructuring of metal surfaces by corrosion for efficient water splitting. *Chem Phys Lett* 2016;644:51–5.
- [35] Wang L, Zhu Y, Zeng Z, Lin C, Giroux M, Jiang L, et al. Platinum-nickel hydroxide nanocomposites for electrocatalytic reduction of water. *Nano Energy* 2017;31:456–61.
- [36] Yin H, Zhao S, Zhao K, Muqsit A, Tang H, Chang L, et al. Ultrathin platinum nanowires grown on single-layered nickel hydroxide with high hydrogen evolution activity. *Nat Commun* 2015;6:6430.
- [37] Gusieva K, Davies CHJ, Scully JR, Birbilis N. Corrosion of magnesium alloys: the role of alloying. *Int Mater Rev* 2015;60:169–94.
- [38] Medeiros MG, Bessette RR, Deschenes CM, Atwater DW. Optimization of the magnesium-solution phase catholyte semi-fuel cell for long duration testing. *J Power Sources* 2001;96:236–9.
- [39] Cheng YL, Qin TW, Wang HM, Zhang Z. Comparison of corrosion behaviors of AZ31, AZ91, AM60 and ZK60 magnesium alloys. *T Nonferr Metal Soc* 2009;19:517–24.
- [40] Liu LJ, Schlesinger M. Corrosion of magnesium and its alloys. *Corros Sci* 2009;51:1733–7.
- [41] Zhao MC, Schmutz P, Brunner S, Liu M, Song GL, Atrens A. An exploratory study of the corrosion of Mg alloys during interrupted salt spray testing. *Corros Sci* 2009;51:1277–92.
- [42] Zhao MC, Liu M, Song GL, Atrens A. Influence of the beta-phase morphology on the corrosion of the Mg alloy AZ91. *Corros Sci* 2008;50:1939–53.
- [43] Hiroi M. Pressure effects on the performance and the emf of the Mg-AgCl seawater battery. *J Appl Electrochem* 1980;10:203–11.
- [44] Giovanelli D, Lawrence NS, Compton RG. Electrochemistry at high pressures: a review. *Electroanal* 2004;16:789–810.